European Journal of Nuclear Medicine and Molecular Imaging
https://doi.org/10.1007/s00259-026-07931-1

ORIGINAL ARTICLE

Diagnostic impact of interpretation criteria for [^{18}F]PSMA-1007 PET/CT: Prospective comparison with CT and bone scan

Yuwei Liu[1] · Koji Hatano[2] · Motohide Uemura[3] · Takero Hirata[4] · Sadahiro Naka[5,6] · Kenta Kurimoto[5,6] · Hidetaka Sasaki[7] · Takashi Kamiya[7] · Ryo Aihara[5] · Feier Ding[5] · Jens Cardinale[8] · Frederik L. Giesel[8,9] · Rudolf A. Werner[10] · Daisuke Katayama[5] · Hiroki Kato[9] · Kayako Isohashi[5] · Noriyuki Tomiyama[5,9] · Norio Nonomura[2] · Tadashi Watabe[1,5]

Received: 16 January 2026 / Accepted: 7 May 2026

Abstract

Purpose The PSMA Reporting and Data System (PSMA-RADS) has been proposed to standardize the interpretation of PSMA-PET. However, its diagnostic performance has not been fully validated. This study aimed to determine the optimal interpretation criteria for PSMA-PET and to compare its diagnostic performance with conventional imaging.

Methods This prospective study enrolled 284 patients across various disease stages who underwent [^{18}F]PSMA-1007 PET/CT. Diagnostic performance was evaluated using different positivity thresholds based on PSMA-RADS categories, PSMA-expression scores, and SUVmax, and was compared with that of CT and bone scan (BS). True-positive rates were summarized across PSMA-RADS categories.

Results A total of 771 lesions were analyzed. PSMA-RADS demonstrated superior diagnostic performance compared with other interpretation criteria. Using PSMA-RADS-4 as the positivity threshold, [^{18}F]PSMA-1007 PET/CT achieved a sensitivity of 78.5% and a specificity of 95.3%. PSMA-RADS-3 increased sensitivity to 98.4% but reduced specificity to 58.8%. PSMA-expression score 2 yielded a sensitivity of 52.2% and a specificity of 99.3%, whereas SUVmax cutoff of 5.7 yielded a sensitivity of 72.6% and a specificity of 85.8%. When PSMA-RADS-4 was used as the positivity threshold, PET/CT showed higher sensitivity than CT (81.3% vs. 48.6%) and BS (84.5% vs. 65.7%), as well as higher accuracy (83.2% vs. 56.2% and 87.6% vs. 74.5%, respectively). The true-positive rate of PSMA-RADS-3 lesions was 69.7%, which was substantially lower than that of PSMA-RADS-4 lesions (96.7%).

Conclusion PSMA-RADS-4 represents an optimal positivity threshold for [^{18}F]PSMA-1007 PET/CT, providing superior diagnostic performance compared with CT and BS and supporting its clinical utility for standardized image interpretation.

Keywords Prostate cancer · [^{18}F]PSMA-1007 · PET/CT · PSMA-RADS · Positivity threshold

✉ Yuwei Liu
liu.yuwei.cer@osaka-u.ac.jp

✉ Tadashi Watabe
watabe.tadashi.med@osaka-u.ac.jp

[1] Laboratory for Theranostics, Division of Clinical Translation, Institute for Radiation Sciences, The University of Osaka, 1-10 Yamadaoka, Suita, Osaka 565-0871, Japan

[2] Department of Urology, Graduate School of Medicine, The University of Osaka, Suita, Japan

[3] Department of Urology, Fukushima Medical University School of Medicine, Fukushima, Japan

[4] Department of Radiation Oncology, Graduate School of Medicine, The University of Osaka, Suita, Japan

[5] Department of Radiology, Graduate School of Medicine, The University of Osaka, Suita, Japan

[6] Department of Pharmacy, The University of Osaka Hospital, Suita, Japan

[7] Department of Medical Technology, The University of Osaka Hospital, Suita, Japan

[8] Department of Nuclear Medicine, Medical Faculty, University Hospital Duesseldorf, Heinrich-Heine-University Duesseldorf, Düsseldorf, Germany

[9] Institute for Radiation Sciences, The University of Osaka, Suita, Japan

[10] Department of Nuclear Medicine, Ludwig-Maximilians-Universität München, München, Germany

Published online: 22 May 2026

Introduction

Prostate cancer (PCa) is one of the most common solid malignancies in men [1, 2], and despite the central role of radiological evaluation in the disease staging and treatment decision-making, accurate lesion characterization remains challenging in clinical practice [3]. Prostate-specific membrane antigen (PSMA) is highly expressed in PCa cells and PSMA-targeted positron emission tomography/computed tomography (PSMA PET/CT) enables visualization of tumor uptake even in the absence of overt morphologic changes. Among approved PSMA-targeted radiotracers, [^{18}F]PSMA-1007 offers low urinary excretion, reduced pelvic background, higher-resolution PET imaging and improved availability compared with ^{68}Ga-labeled PSMA tracers [4]. Overall, PSMA PET/CT has demonstrated higher diagnostic accuracy than conventional imaging modalities, including CT and bone scan (BS), and has increasingly become important in PCa evaluation [5–7]. Furthermore, PSMA expression can also be observed in tumor-associated neovasculature, potentially contributing to the detection of other malignancies, such as breast cancer [8]. Nevertheless, PSMA expression is not entirely specific to tumor lesions and can also be observed in normal tissues or benign lesions, therefore, the clinical utility of PSMA PET/CT may be influenced by the selection of positivity thresholds [2].

With the expanding clinical use of PSMA PET/CT, various interpretation criteria have been proposed, including the PSMA Reporting and Data System (PSMA-RADS), the Prostate Cancer Molecular Imaging Standardized Evaluation (PROMISE), E-PSMA and semi-quantitative metrics such as the maximum standardized uptake value (SUVmax) [9–11]. However, a unified definition of PET positivity remains lacking [3, 12]. Variable application of positivity thresholds leads to differences in reported sensitivity and specificity [9, 13–15]. Moreover, limited agreement among interpretation criteria complicates cross-study comparisons and clinical decision-making [3, 16]. Although the recently published Standardized PSMA PET/CT Analysis and Reporting Consensus reflects expert agreement supporting the reporting of diagnostic certainty according to PSMA-RADS [17], equivocal lesions remain common and their optimal interpretation remains controversial.

Therefore, this prospective study aimed to determine the optimal interpretation criteria for [^{18}F]PSMA-1007 PET/CT, evaluate the impact of threshold selection on lesion classification, and compare its diagnostic performance with conventional imaging.

Methods

Patients

This prospective study enrolled 289 consecutive patients with PCa who underwent [^{18}F]PSMA-1007 PET/CT at the University of Osaka Hospital between Sep 2019 and Feb 2024. The inclusion criteria were as follows: (1) newly diagnosed PCa undergoing metastasis screening; (2) recurrent PCa after definitive treatment (surgery or radiotherapy) with an elevated prostate-specific antigen (PSA) level, including biochemical recurrence (BCR) and hormone-sensitive prostate cancer (HSPC) patients; (3) non-metastatic castration-resistant prostate cancer (nmCRPC) patients receiving androgen receptor pathway inhibitors (ARPI); (4) metastatic castration-resistant prostate cancer (mCRPC) patients with metastatic disease confirmed by CT and/or BS. Patients unable to maintain stable positioning during imaging or considered unsuitable by investigators were excluded. Some patients underwent repeat [^{18}F]PSMA-1007 PET/CT examinations for follow-up and were categorized as the follow-up group.

The study was approved by the institutional review board of the University of Osaka Hospital (approval number: 19066).

Imaging procedures

[^{18}F]PSMA-1007 was synthesized using an MPS200 module (Sumitomo Heavy Industries) as previously reported [18]. The PET/CT scans (from the vertex to mid-thigh) were performed 60 min after intravenous injection of [^{18}F]PSMA-1007 (248.8 ± 32.8 MBq) on a Discovery 710 (GE Healthcare, Milwaukee, United States) with 3D acquisition (192 × 192 matrix; 3.65 mm pixel; 2 min/bed). Reconstruction used ordered-subset expectation maximization algorithm (three iterations, eight subsets) with Gaussian smoothing to a 4-mm transaxial resolution at full width at half maximum. Attenuation correction was based on low-dose non-contrast CT (100 mA), reconstructed at 3.75 mm thickness with 3.27 mm increments. Diagnostic CT and/or BS were performed in accordance with standard institutional procedures. The interval between CT/BS and PSMA PET/CT was set within ± 3 months.

Imaging analysis

All PSMA PET/CT and BS images were initially interpreted by one board-certified nuclear medicine physician and subsequently reviewed by a second board-certified nuclear medicine physician; any discrepancies were resolved by consensus. Diagnostic CT images were evaluated by a

radiologist. For each PSMA PET/CT examination, all lesions with visually increased uptake were recorded and categorized as local, lymph node (LN), bone, or other metastases. Lesions were evaluated using three analytic criteria: PSMA-RADS, PSMA-expression score, and SUVmax.

PSMA-RADS: According to PSMA-RADS v2.0, lesions were categorized as: PSMA-RADS-1: definitively benign, PSMA-RADS-2: likely benign, PSMA-RADS-3 (including 3 A, 3B, 3 C, and 3D): equivocal, PSMA-RADS-4: high uptake without corresponding anatomic abnormality, PSMA-RADS-5: high uptake with corresponding anatomic abnormality, PSMA-RADS-5T: treated prior metastases [9].

PSMA-expression score: According to PROMISE v2, PSMA uptake was graded by comparing lesion SUVmax with reference organ uptake. Score 0: uptake ≤ blood pool, Score 1: uptake > blood pool but ≤ spleen, Score 2: uptake > spleen but ≤ parotid gland, Score 3: uptake > parotid gland [10]. The mean standardized uptake value (SUVmean) of the blood pool, spleen, and parotid gland was measured using spherical region of interest (ROI) (1.5–2 cm in the descending aorta and 2–3 cm in the spleen and parotid gland).

SUVmax: Quantitative measurements were obtained by placing a spherical ROI over each lesion to derive SUVmax values.

Focal bone uptake higher than the blood pool but not exceeding twice the blood pool activity, without corresponding CT finding, was defined as unspecified bone uptake (UBU) in this study. The number and distribution of UBU were recorded separately.

Reference standard of true positive lesions

A lesion on [^{18}F]PSMA-1007 PET was classified as a true positive lesion if it met at least one of the following criteria:

(1) Histopathologic confirmation;
(2) Concordant findings on other imaging modalities (CT, MRI, or BS);
(3) Decreased uptake in response to treatment or increased uptake due to progression;
(4) Morphological changes on follow-up imaging (e.g., appearance of osteosclerosis on CT);
(5) PSA decline after radiotherapy to the lesion without systemic treatment;
(6) High-uptake in LN regardless of enlargement. High uptake in LN was defined as SUVmax ≥ 5.0, using blood-pool activity as the reference.

Based on the reference standard, each lesion was classified as positive, negative, or indeterminate.

Data analysis

Receiver operating characteristic (ROC) curve analysis was performed at the lesion level to compare the diagnostic performance of PSMA-RADS, PSMA-expression score, and SUVmax, with pairwise comparisons conducted using the DeLong test. For SUVmax, optimal cutoff value was determined using the Youden index (sensitivity + specificity − 1). Sensitivity, specificity, and accuracy of PSMA PET/CT were evaluated using different positivity thresholds based on PSMA-RADS, PSMA-expression score and SUVmax, and diagnostic performance was compared with diagnostic CT and BS using the McNemar test.

True positive rates of different PSMA-RADS and PSMA-expression score categories were compared in all patients. In BCR patients, the lesion-level detection rates among true positive lesions were compared across PSA levels using PSMA-RADS-3 and −4 as positivity criterion. χ^2 tests were used for group comparisons. In nmCRPC patients, metastatic detection by PET/CT was summarized. In mCRPC patients, regional detection efficacy of PET/CT, diagnostic CT and BS were compared using the McNemar test, with PET/CT results evaluated using both PSMA-RADS-3 and −4 thresholds.

Statistical analysis

Statistical analyses were performed using Excel software (version 16.50), SPSS software (version 27.0.1) and R software (version 4.5.2). p values < 0.05 were considered statistically significant.

Results

Patients

Of 289 enrolled patients, 284 were analyzed after exclusion of cases with small-cell carcinoma and missing imaging data. Histopathologic confirmation was available in 21.8% patients (62/284). Clinical characteristics are summarized in Table 1. Among these patients, 181 underwent additional diagnostic CT and 218 underwent BS, with a median interval of 27 days between PET/CT and CT (IQR 11–47; range 0–90) and 28 days between PET/CT and BS (IQR 13–48; range 1–92).

Diagnostic performance according to different criteria

A total of 873 lesions were identified, including 139 local lesions (23 primary and 116 local recurrence), 301 LN

Table 1 Clinical characteristics of patients

Characteristics	Value
Patients (*n*)	284
Age (yr), median (IQR)	72(67–76)
PSA (ng/mL), median (IQR)	2.58 (0.755–5.805)
Status (*n*)	
Primary staging	23
BCR	145
HSPC	28
nmCRPC	19
mCRPC	20
Follow-up	47
Others	2
ISUP Gleason grade (*n*)	
1	25
2	47
3	62
4	68
5	74
N.A.	7

N number, *IQR* interquartile range

metastases, 417 bone metastases, and 16 other metastases. Using the predefined reference standard, 623 lesions were classified as positive and 148 as negative, while 102 lesions were indeterminate due to unavailable or insufficient follow-up and were excluded from subsequent analyses. At the lesion level, histopathology verified 7.7% lesions (67/873).

ROC analysis demonstrated that PSMA-RADS achieved the highest diagnostic performance, with an area under curve (AUC) of 0.931, compared with PSMA-expression score (AUC = 0.765) and SUVmax (AUC = 0.828) (Fig. 1a). PSMA-RADS showed significantly higher AUC than the other criteria according to DeLong test (both $p < 0.001$). Subgroup ROC analyses by anatomical regions showed a similar pattern, with PSMA-RADS yielding the highest AUC for both LN and bone lesions (Fig. 1b and c), although the difference between PSMA-RADS and SUVmax for LN lesions was not significant ($p = 0.6698$).

The diagnostic performance of PET/CT was evaluated with different positivity thresholds for PSMA-RADS (PSMA RADS-3 or −4), PSMA-expression score (score 1 or 2) and SUVmax. Using PSMA-RADS-4, the sensitivity of PSMA PET/CT was 78.5% and the specificity was 95.3% (Fig. 2a), whereas PSMA-RADS-3 yielded very high sensitivity (98.4%) but limited specificity (58.8%). Although overall accuracy decreased from 90.8% to 81.7% when equivocal PSMA-RADS-3 lesions were regarded as negative, PSMA-RADS-4 achieved more favorable balance between sensitivity and specificity, reflected by a higher Youden index. Under this threshold, PSMA PET/CT maintained high sensitivity across regions, with particularly high specificity for LN and bone lesions (Table 2).

A similar trend was observed in the PSMA-expression score. Score 1 yielded high sensitivity (97.8%) but

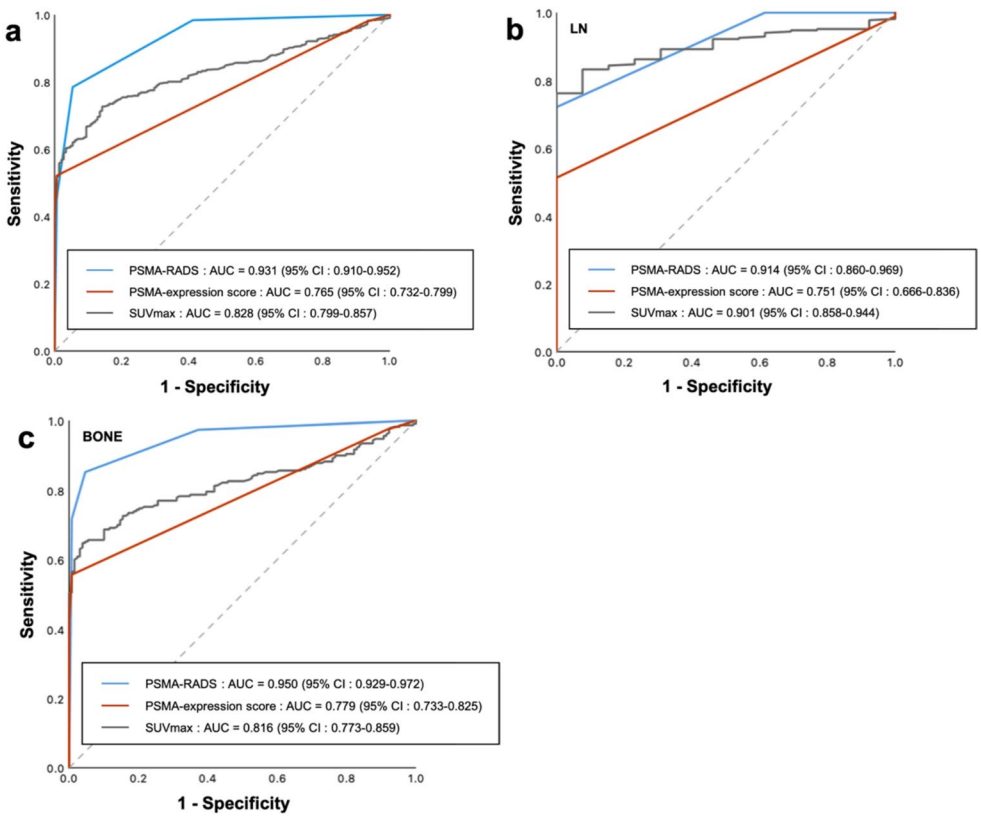

Fig. 1 ROC curves for PSMA RADS, PSMA-Expression Score, and SUVmax for differentiating positive from benign lesions in (**a**) all lesions ($n = 771$), (**b**) LN lesions ($n = 282$), and (**c**) bone lesions ($n = 360$). Dashed diagonal line indicates the reference line representing no discrimination

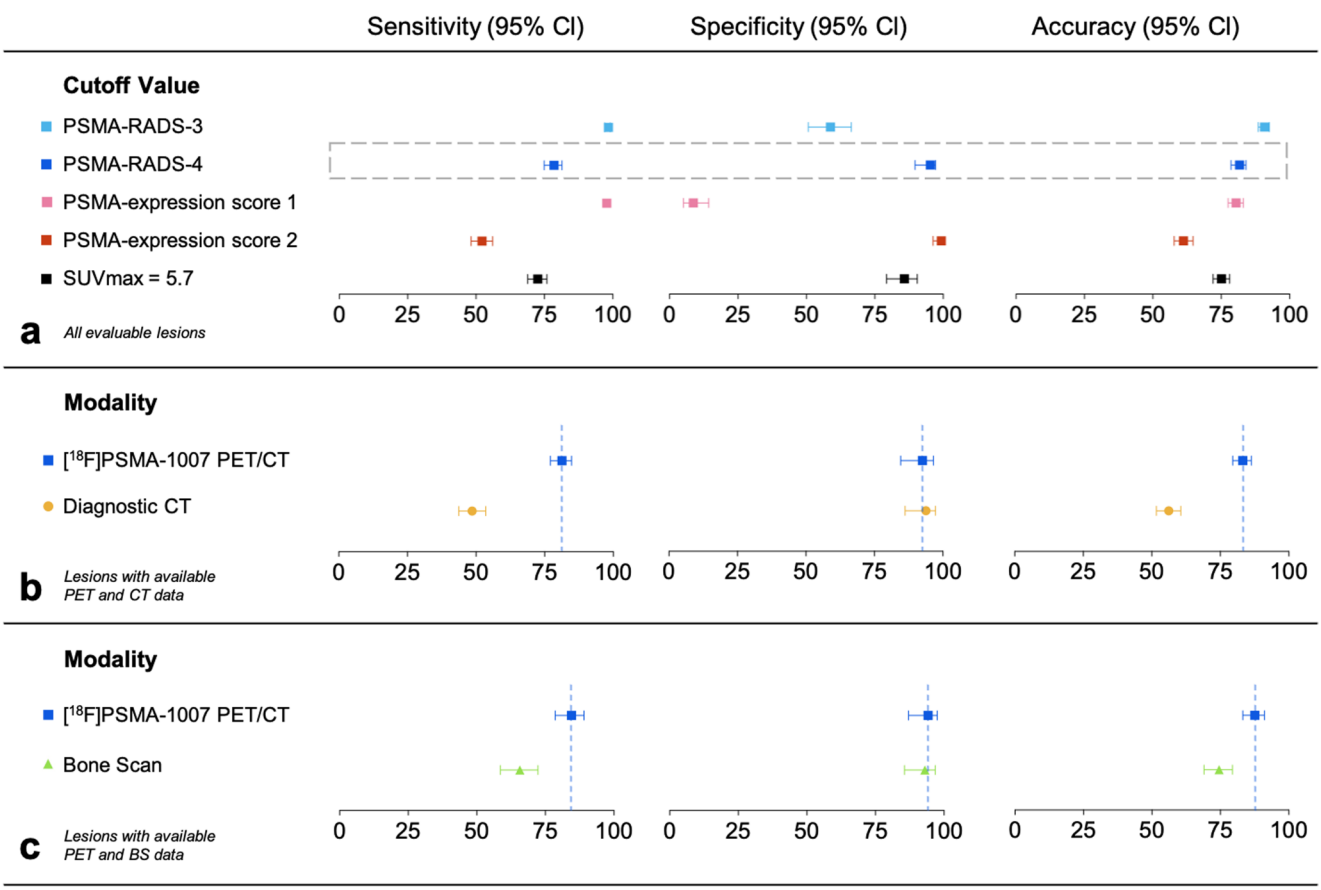

Fig. 2 Diagnostic performance of [^{18}F]PSMA-1007 PET/CT (n=771), diagnostic CT (n=475) and BS (n=267). (**a**) Sensitivity, specificity and accuracy of [^{18}F]PSMA-1007 PET/CT using different positivity thresholds in all evaluable lesions. PSMA-RADS-3 represents the combined results of 3 A-3D. (**b**–**c**) Comparison of [^{18}F]PSMA-1007 PET/CT (PSMA-RADS-4 as positivity cutoff) with CT and BS, respectively, in lesions with paired data. Indeterminate lesions were excluded

Table 2 Sensitivity, specificity, and accuracy of [^{18}F]PSMA-1007 PET/CT in different regions using PSMA-RADS-4 as the positivity threshold. Values are shown as percentage with raw counts in parentheses and 95% confidence intervals in brackets

Region	Sensitivity (%)	Specificity (%)	Accuracy (%)
Local (n=114)	88.3 (98/111) [81.0–93.0]	33.3 (1/3) [6.1–79.2]	86.8 (99/114) [79.4–91.9]
LN (n=282)	72.1 (194/269) [66.5–77.1]	100.0 (13/13) [77.2–100.0]	73.4 (207/282) [68.0–78.2.0.2]
Bone (n=360)	85.3 (197/231) [79.7–88.9]	95.3 (124/129) [90.2–97.9]	88.9 (321/360) [84.9–91.5]

extremely low specificity (7.4%), whereas score 2 markedly improved specificity (99.3%) and reduced the sensitivity (52.2%), accompanied by a lower accuracy (80.4% for score 1 vs. 61.2% for score 2) and a higher Youden index. The Youden-determined optimal SUVmax cutoff value for all lesions was 5.7, corresponding to a sensitivity of 72.6%, specificity of 85.8%, and accuracy of 75.1% (Fig. 2a).

Exploration of SUVmax cutoff values in different regions

To explore the potential utility of quantitative parameter, we calculated the region-specific optimal SUVmax cutoff values and compared with the overall optimal cutoff value.

For LN metastases, lowering the cutoff value from 5.7 to 4.9 significantly increased sensitivity (72.1% to 76.2%, p<0.001) while maintaining 100.0% specificity, resulting in improved accuracy (73.4% to 77.3%). For bone metastases, raising the cutoff value from 5.7 to 8.1 reduced sensitivity (72.3% to 64.5%, p<0.001) but increased specificity (84.5% to 96.1%, p<0.001), with a slight decrease in accuracy (76.7% to 75.8%).

Comparison of [^{18}F]PSMA-1007 PET/CT with CT and BS

Using PSMA-RADS-4 as the diagnostic threshold, lesion-level diagnostic performance of PSMA PET/CT was compared with diagnostic CT and BS in cases with available

paired imaging data (475 lesions with paired PET/CT and CT data and 267 lesions with paired PET/CT and BS data).

PSMA PET/CT demonstrated significantly higher sensitivity than CT and BS (81.3% vs. 48.6% and 84.5% vs. 65.7%, respectively; both $p<0.001$), while specificity was comparable to that of CT (92.5% vs. 93.8%) and BS (94.2% vs. 93.0%), with no statistically significant differences. Accuracy was also higher for PSMA PET/CT compared with CT and BS (83.2% vs. 56.2% and 87.6% vs. 74.5%, respectively) (Fig. 2b and c). Representative comparative cases are shown in Figs. 3 and 4.

True positive lesions across PSMA-RADS and PSMA-expression score

The distribution of positive and negative lesions across PSMA-RADS and PSMA-expression score categories is summarized in Fig. 5, with true positive rates differing significantly across categories (both $p<0.001$).

For PSMA-RADS (Fig. 5a), true positive rates increased from 10.3% (10/97) in PSMA-RADS-2 to 69.7% (124/178) in PSMA-RADS-3, 96.7% (204/211) in PSMA-RADS-4, and 100.0% in PSMA-RADS-5 (228/228) and − 5 T (57/57). A similar ascending pattern was observed in all regions, particularly in bone metastases, with increasing from 6.9% (6/87), to 39.4% (28/71), 86.1% (31/36), and 100.0% (138/138 and 17/17). For equivocal lesions (Fig. 5b), LN lesions classified as PSMA-RADS-3 A showed a high true positive rate (87.1%, 54/62), whereas bone lesions classified as PSMA-RADS-3B demonstrated a lower positive rate (38.6%, 27/70). Representative examples of PSMA-RADS-2, −3 A, −3B, −4, and − 5 lesions are shown in Supplementary Fig. 1–4.

PSMA-expression score showed a comparable trend (Fig. 5c), with positive rates of 56.0% (14/25) and 67.6% (284/420) for Score 0 and Score 1, increasing to 98.9% (86/87) for Score 2 and 100.0% (239/239) for Score 3. Bone lesions showed similar score-dependent increase in positivity. In addition, 43 patients showed higher SUVmean of spleen than the parotid gland and were therefore directly classified as PSMA-expression score 3.

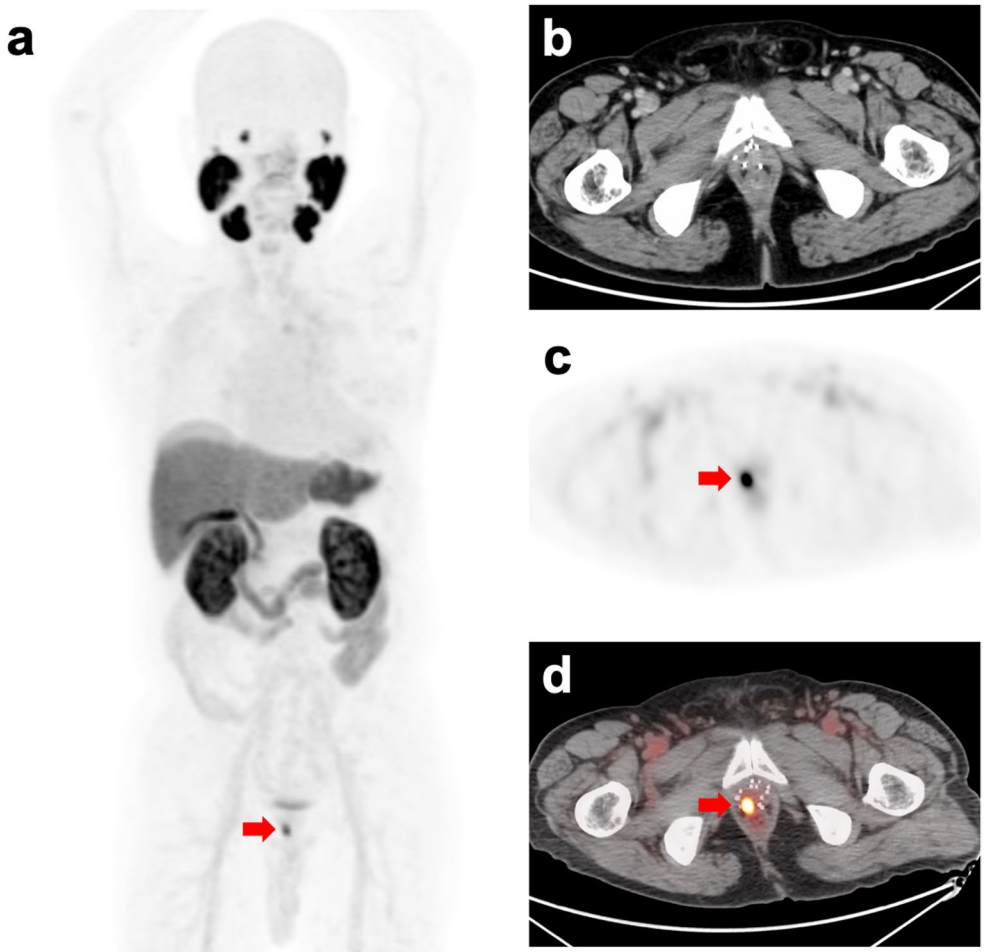

Fig. 3 Representative images from a patient who underwent ^{125}I-seed implantation, with PSA level rising to 2.63 ng/mL after 9 years of follow-up. (**a**) Maximum-intensity projection of [^{18}F]PSMA-1007 PET shows focal tracer uptake (arrows). (**b**) Corresponding CT image. (**c**) Transaxial PET and (**d**) fused PET/CT localize uptake to the prostate bed (arrows). Histopathology confirmed local recurrence. The patient underwent stereotactic body RT targeting the PSMA-positive lesion (36 Gy in 6 fractions), resulting in PSA level reduction to 0.05 ng/mL at 8 months after RT. *RT*, radiation therapy

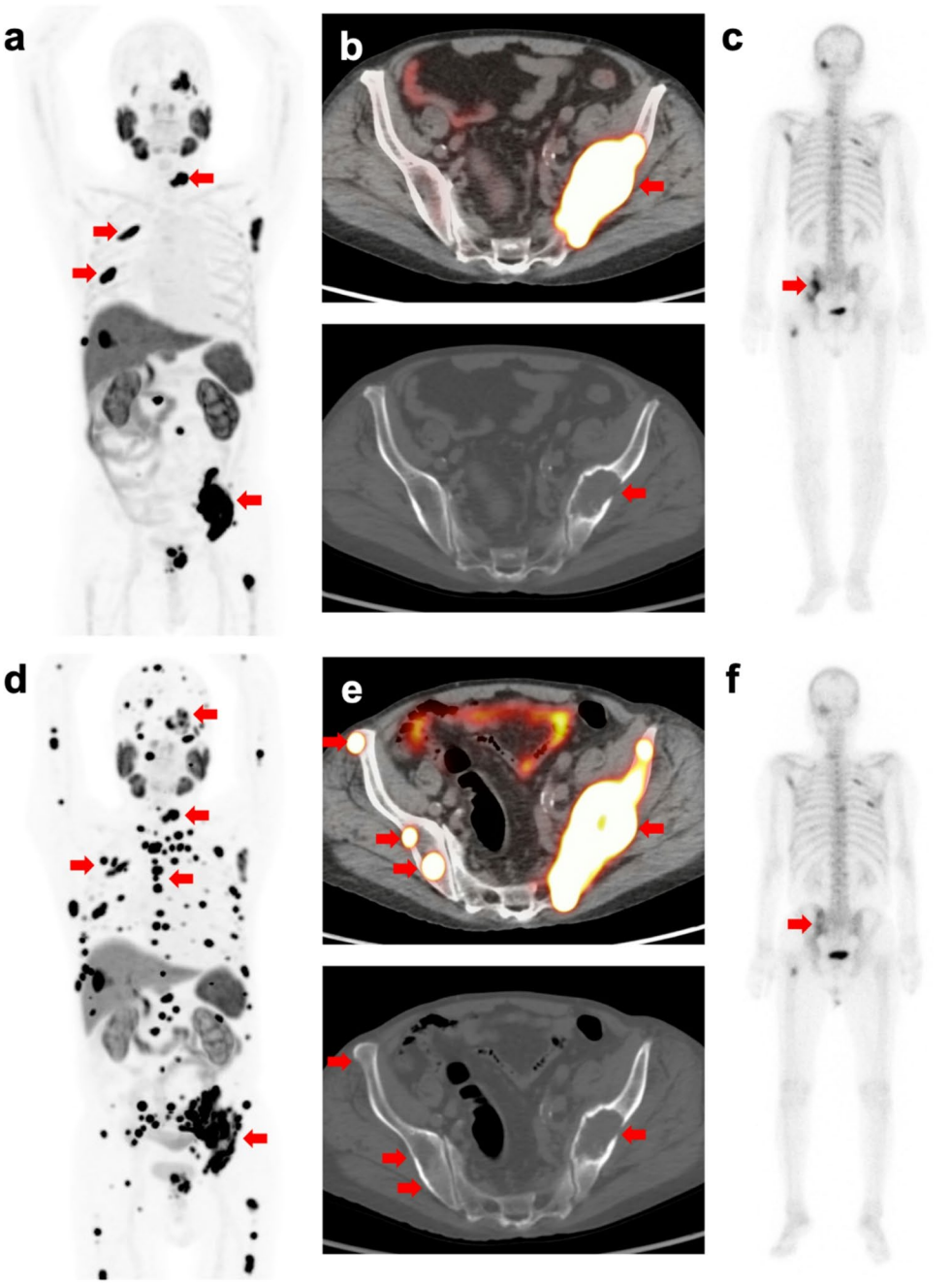

Fig. 4 Representative images from a mCRPC patient undergoing cabazitaxel therapy. (**a**–**c**) Baseline imaging: (a) MIP of [^{18}F]PSMA-1007 PET shows intense uptake in multiple skeletal lesions (arrows). (**b**) Fused PET/CT (top) and CT (bottom) images demonstrate focal uptake with CT changes in the left iliac bone (arrow). (**c**) Posterior BS shows uptake in the corresponding lesion. (**d**–**f**) Follow-up imaging at 6 months, with PSA levels increasing from 420.22 to 983.61 ng/mL. (**d**) MIP demonstrates disease progression with more extensive uptake. (**e**) PET/CT fusion image shows increased uptake in the left iliac bone and new uptake in the right iliac bone, without CT progression (arrow). (**f**) BS shows reduced uptake, without new lesions, suggesting delayed response of CT and BS relative to PSMA PET/CT

PSA-stratified detection rates in BCR patients

A total of 193 true-positive lesions were included for PSA-stratified detection rate analysis, with PSA grouped as ≤0.2, 0.2–0.5, 0.5–1, 1–2, and >2 ng/mL.

In the PSA≤0.2 ng/mL group, only one lesion was present, and the detection rate was 100.0% for both PSMA-RADS-3 and −4. Using PSMA-RADS-3 as PET positive standard, detection rates remained uniformly high across PSA levels (95.0% at PSA 0.2–0.5 ng/mL, 100.0% at PSA 0.5–1 ng/mL and 1–2 ng/mL, and 95.4% at PSA>2 ng/mL). In contrast, PSMA-RADS-4 demonstrated a PSA-dependent increase in detection rates ($p<0.001$), from 40.0% (8/20) at PSA 0.2–0.5 ng/mL to 42.9% (9/21) at 0.5–1 ng/mL, 65.0% (13/20) at 1–2 ng/mL, and 77.1% (101/131) at >2 ng/mL (Fig. 6a).

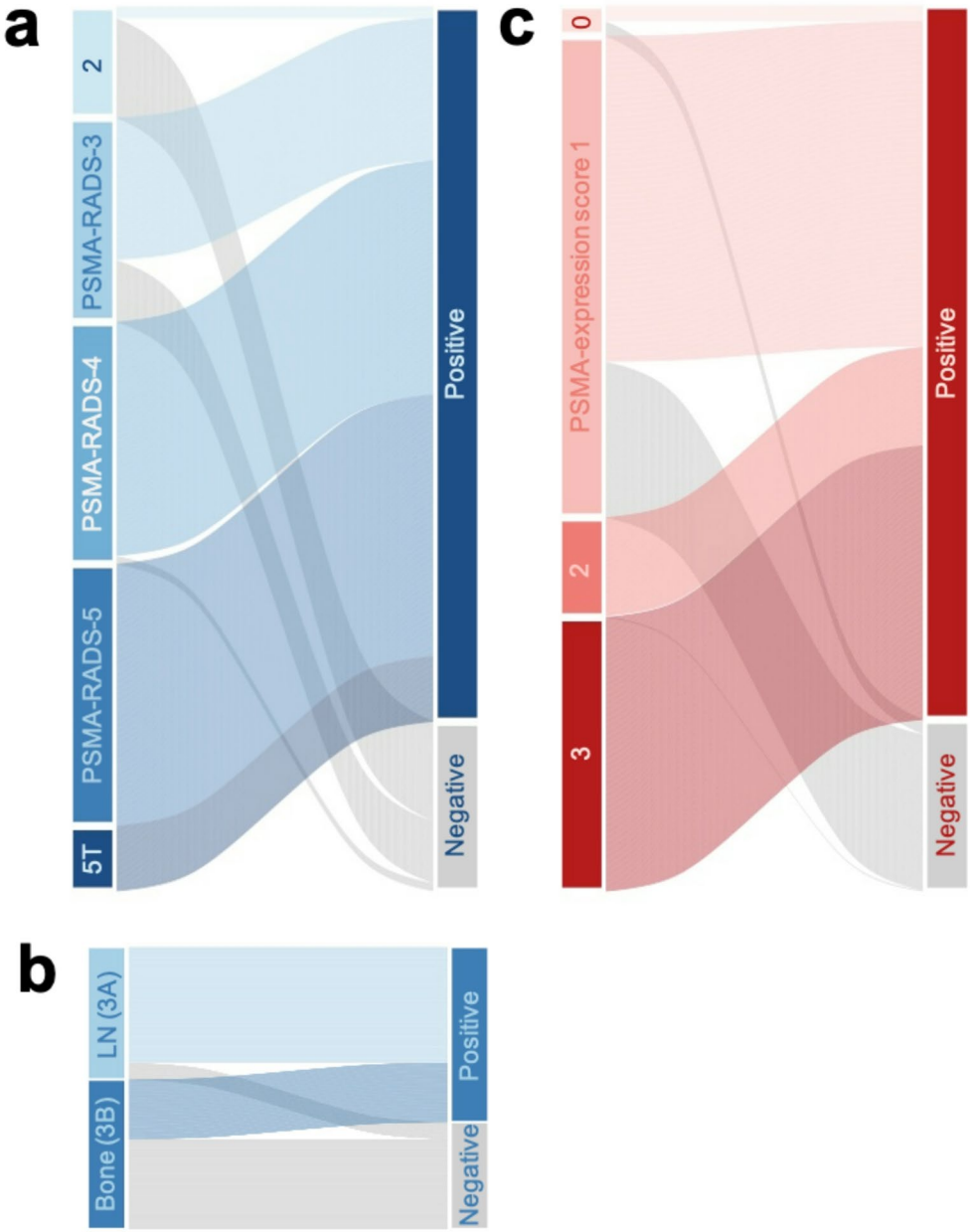

Fig. 5 Distribution of positive and negative lesions across (**a**) PSMA-RADS categories: PSMA-RADS-2 ($n=97$), PSMA-RADS-3 ($n=178$), PSMA-RADS-4 ($n=211$), PSMA-RADS-5 ($n=228$), and PSMA-RADS-5T ($n=57$), (**b**) equivocal LN lesions classified as PSMA-RADS-3 A ($n=62$) and bone lesions classified as PSMA-RADS-3B ($n=70$), and (**c**) PSMA-expression score categories: score 0 ($n=25$), score 1 ($n=420$), score 2 ($n=87$), and score 3 ($n=239$). Indeterminate lesions were excluded

Metastatic detection on PET/CT in nmCRPC patients and performance comparison of PET/CT, CT, and BS in mCRPC patients

In 19 patients with nmCRPC, [^{18}F]PSMA-1007 PET/CT identified local recurrence in 12 patients (63.2%) and metastatic lesions in 6 patients (31.6%), including pelvic LN metastases in 2 (10.5%), distant LN metastases in 2 (10.5%), and bone metastases in 4 (21.1%).

In mCRPC patients, lesion-level detection rate of PSMA PET/CT was compared with CT and BS using paired imaging data (69 lesions with paired PET/CT and CT data and 40 lesions with paired PET/CT and BS data).

For lesions with paired PSMA PET/CT and CT data, PET/CT detected all lesions using PSMA-RADS-3 as the positive threshold. Using PSMA-RADS-4, PET/CT detected 3/3 local lesions (100.0%), 16/19 LN lesions (84.2%), and 41/46 bone lesions (89.1%), whereas CT detected 2/3 local lesions (66.67%), 11/19 LN lesions (57.9%), and 37/46 bone lesions (80.4%) (Fig. 6b). Although detection rates were higher for PSMA PET/CT in LN and bone lesions, differences were not statistically significant by the McNemar test ($p=0.125$ and $p=0.289$, respectively). For lesions with PET/CT and BS data, PET/CT detected 40/40 lesions (100%) using PSMA-RADS-3 and 35/40 lesions (87.5%) using PSMA-RADS-4. Meanwhile, BS detected 26/40 lesions (65.0%),

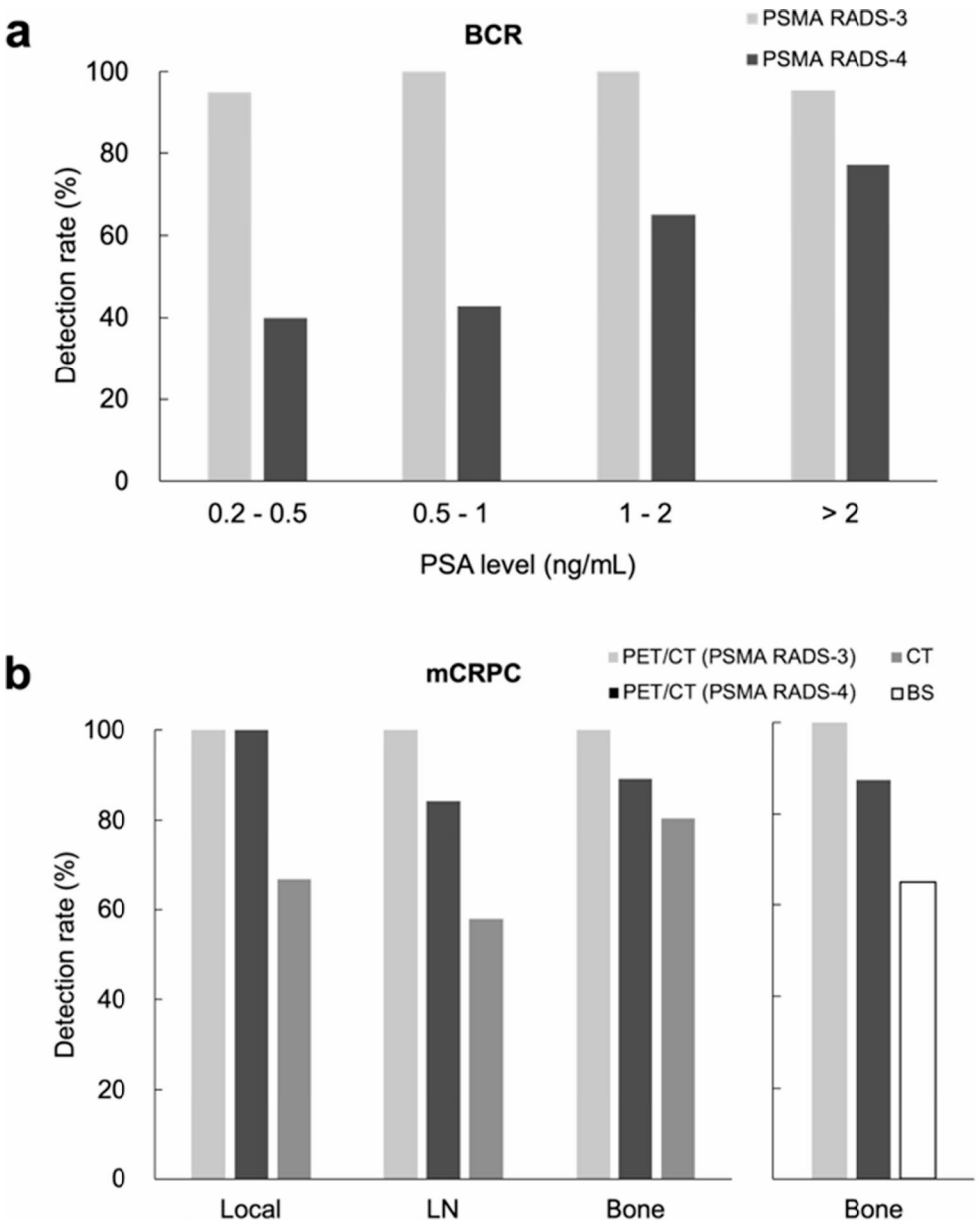

Fig. 6 Lesion-level detection rates of [^{18}F]PSMA-1007 PET/CT (**a**) stratified by PSA level in BCR patients (PSA 0.2–0.5 ng/mL, $n=20$; 0.5–1 ng/mL, $n=21$; 1–2 ng/mL, $n=20$; >2 ng/mL, $n=131$), and (**b**) comparison with diagnostic CT ($n=69$) and BS ($n=40$) across different lesions in mCRPC patients, using PSMA-RADS-3 and PSMA-RADS-4 positivity thresholds

resulting in a significantly higher detection rate for PET/CT under the PSMA-RADS-4 threshold ($p=0.004$).

Frequency and distribution of UBU

At patient-level, UBU was observed in all stages. The frequencies were 56.5% (13/23) in primary staging, 61.4% (89/145) in BCR, 64.3% (18/28) in HSPC, 63.2% (12/19) in nmCRPC, 40.0% (8/20) in mCRPC, 55.3% (26/47) in the follow-up group, and 100% (2/2) in the others group, with an overall frequency of 59.2% (168/284), defined as having at least one UBU lesion. UBU occurred most in the ribs (50.4%, 143/284), followed by the spine (21.5%, 61/284) and pelvis (15.1%, 43/284) (Fig. 7a), with a similar distribution across disease stages (Fig. 7b).

Discussion

The primary purpose of this study was to identify an optimal positivity threshold for evaluating the diagnostic performance of [^{18}F]PSMA-1007 PET/CT as well as compare the diagnostic accuracy with conventional imaging (CT and BS) in patients with various stages of PCa.

We systematically evaluated the diagnostic performance of [^{18}F]PSMA-1007 PET/CT using different positivity criteria, including PSMA-RADS, PSMA-expression score, and SUVmax. As a result, PSMA-RADS demonstrated the highest AUC on ROC analysis, indicating superior performance compared with other criteria. The advantage may come from the integration of tracer uptake intensity and lesion

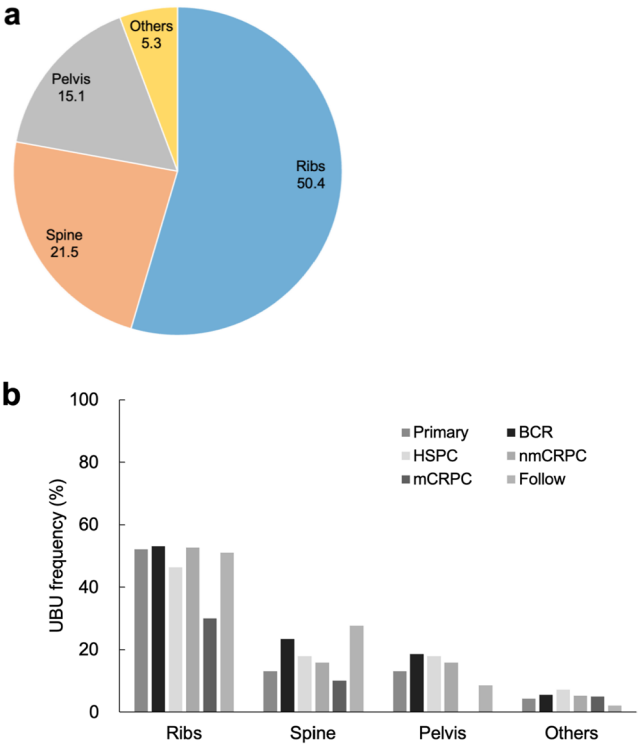

Fig. 7 UBU frequency at patient-level in (**a**) overall anatomical distribution ($n=284$) and (**b**) across disease stages (primary staging, $n=23$; BCR, $n=145$; HSPC, $n=28$; nmCRPC, $n=19$; mCRPC, $n=20$; follow-up, $n=47$)

characteristics within PSMA-RADS, but the evaluation essentially depends on relative visual judgment rather than fixed numerical thresholds, which may introduce reader-dependent variability and potentially affect the standardization and reproducibility. Additionally, the PSMA-expression score is defined according to PROMISE V2, which is a framework for standardizing the imaging diagnosis, staging, and treatment response evaluation of PCa based on PSMA-PET. Although it was used for evaluation of eligibility and monitoring of treatment response in ^{177}Lu-PSMA radioligand therapy rather than for malignancy discrimination, the PSMA-expression score was included in the present study because of its simplicity and wide clinical use [10]. Subsequently, we examined the impact of different positivity thresholds within each interpretation criterion, with particular attention to the equivocal lesions. In our study, changing the positivity threshold from PSMA-RADS-3 to −4, which means classifying equivocal lesions as negative, as well as from PSMA-expression score 1 to score 2 was associated with decreased sensitivity and increased specificity. Yin et al. used [^{68}Ga]PSMA-11 PET for bone metastases, and reported that applying PSMA-RADS-3B cutoff yielded a sensitivity of 100% but a specificity of 63.6%, whereas using PSMA-RADS-4 cutoff increased specificity to 100% and decreased sensitivity to 40.5% [19, 20]. In region-specific analyses, PSMA-RADS-4 showed favorable diagnostic efficacy for both LN and bone metastases, consistent with prior findings that at least PSMA-RADS-4 is required to classify bone lesions as positive [2]. For local lesions, they are associated with heterogeneous background conditions, including treatment-naive primary lesions, post-radical prostatectomy status, and post-radiation therapy, we did not include them in the comparison of diagnostic criteria. In addition, although specificity for local lesions was relatively low in the present study, it may be limited by the small sample size in this subgroup (false positive = 2, true negative = 1), while the high sensitivity remains clinically meaningful. Notably, our findings are based on [^{18}F]PSMA-1007, and the same thresholds may not apply to other PSMA tracers with different biodistribution and background uptake.

Beyond threshold-based performance, true positive rates increased with higher PSMA-RADS and PSMA-expression score categories across both overall and different regions, consistent with higher malignancy rates for PSMA-RADS-4/5 lesions reported previously [20, 21]. It should be noted that PSMA-RADS-3 lesions exhibited marked regional heterogeneity. In the present study, PSMA-RADS-3 A LN lesions showed higher true positive rate than PSMA-RADS-3B bone lesions, consistent with previously reported malignancy rates of 75% and 21.4%, respectively [20]. Of note, the slightly higher overall true-positive rate of PSMA-RADS-3 A/3B lesions observed in our study may relate to the use of PSMA-RADS version 2.0, which provides general notes on typical manifestations and specifically highlights low-level, CT-negative bone uptake frequently seen with [^{18}F]PSMA-1007 as potentially appropriate for PSMA-RADS-2 [22].

The regional heterogeneity prompted further consideration of the appropriateness of a single SUVmax cutoff value. Although SUVmax can provide supportive quantitative information, it is affected by multiple factors, including difference in PET probes, generation of PET scanners, and PET reconstruction parameters, making it difficult to set a universal threshold across centers [19]. Previous studies have reported different optimal SUVmax cutoff values, such as 5.30 for [^{68}Ga]Ga-PSMA-11 PET and 8.3 for [^{18}F]PSMA-1007 PET, both differing from the present study [14, 23]. Our region-specific analyses revealed that Youden-selected SUVmax cutoff values differed between LN and bone metastases. While LN metastases may benefit from more sensitive detection, bone lesions require threshold to reduce unspecific uptake, suggesting that SUVmax cutoff should be applied cautiously in different regions. Jiao et al. showed that different SUVmax cutoffs were required for peripheral and central prostate lesions, underscoring region-specific SUVmax thresholds even within the same organ

[13]. The PRIMARY score provides a standardized visual assessment of intraprostatic PSMA-PET uptake in the early diagnosis of PCa, with a score of 5 indicating very intense uptake (SUVmax ≥ 12), while other scores are based on the relative uptake, location and morphological characteristics of the uptake, rather than absolute SUVmax values [24]. Overall, these findings suggest that SUVmax may be more suitable as an adjunctive parameter. Meanwhile, Werner et al. mentioned that although PSMA-RADS can be combined with quantitative metrics, further validation is required to define the most suitable SUVmax parameters, supporting integration with structured interpretation systems such as PSMA-RADS [9].

After establishing PSMA-RADS-4 as the optimal diagnostic threshold, [^{18}F]PSMA-1007 PET/CT demonstrated higher sensitivity and accuracy compared with CT and BS, consistent with previous studies in different disease stages [5, 25–27]. Although specificity was slightly lower than CT, it was not significant. It was particularly evident when metastatic disease remained inapparent on conventional imaging, with [^{18}F]PSMA-1007 PET/CT detecting lesions in BCR patients at low PSA levels, and identifying metastatic lesions in 31.6% of nmCRPC patients previously classified as non-metastatic. Similarly, PSMA PET/CT exclusively detected at least one true-positive lesion in approximately 52% of HSPC patients (data not shown), further supporting its value for precise disease assessment when conventional imaging is inconclusive. Furthermore, PSMA PET/CT maintained high diagnostic performance across different regions, especially high specificity for LN and bone lesions, consistent with findings reported in previous studies [28, 29].

Threshold selection consistently influenced detection rates across disease stages. Using PSMA-RADS-3 yielded uniformly high detection rates in both BCR and mCRPC patients, without clear PSA-dependent trend in BCR patients. This suggests potential overestimation at low PSA levels when equivocal lesions are considered positive. In contrast, PSMA-RADS-4 restored a clearer PSA-dependent increase in detection rates, consistent with our previous research and other patient-level studies [18, 26, 30, 31]. In mCRPC patients, PSMA PET/CT outperformed CT and BS even with PSMA-RADS-4 as the positivity criterion, supporting PSMA-RADS-3 as a screening threshold and PSMA-RADS-4 as more suitable for reflecting disease progression risk and treatment decisions. Interpretation at PSA < 0.2 ng/mL was limited by small lesion numbers, while previous studies indicate PSMA PET/CT retains detectability at very low PSA levels [32].

UBU was observed across disease stages, most frequently in the ribs, spine, and pelvis, consistent with previous studies and suggesting that UBU should be carefully considered when interpreting PSMA PET/CT, especially for isolated low-level bone uptake without a CT correlate. During follow-up, we found that 24 of 168 patients with UBU (14.3%) were classified as malignant at the patient level, defined as having at least one UBU lesion classified as true positive, although outcome assessment was not available in all cases. Meanwhile, consideration of the typical anatomic distribution of UBU on [^{18}F]PSMA-1007 may also help avoid interpreting these findings as metastases [33, 34].

This study has several limitations. First, this was a single-center analysis. Second, histopathologic confirmation was not available for all lesions, instead, composite reference standard was used, which may introduce uncertainty and bias estimates of diagnostic performance. This issue will need to be further validated and confirmed in future studies. Third, we only focused on [^{18}F]PSMA-1007, and results of other tracers might be different and remains to be explored. Fourth, this study was based on imaging at 60 min after tracer injection; therefore, the positivity thresholds may not be directly applicable at later time points. Fifth, inter-reader agreement (e.g., κ statistics) was not assessed for PSMA-RADS interpretation, which may limit the reproducibility of our findings.

Conclusion

This prospective study demonstrated that interpretation criteria and positivity thresholds strongly influence PSMA PET/CT performance, with PSMA-RADS-4 providing an appropriate positivity threshold for [^{18}F]PSMA-1007 PET/CT by balancing sensitivity and specificity. Under this threshold, [^{18}F]PSMA-1007 PET/CT outperformed CT and BS, supporting its clinical utility in PCa management.

Supplementary Information The online version contains supplementary material available at https://doi.org/10.1007/s00259-026-07931-1.

Author contributions Conceptualization: YL, FLG, and TW. Data collection: YL, KH, MU, TH, SN, KK, HS, TK, RA, FD, DK, HK, KI, and TW. Formal analysis: YL and TW. Original draft preparation: YL. Review and editing: JC, FLG, RAW, and TW. Supervision: FLG, NT, NN, and TW. All authors have read and agreed to the final version of the manuscript.

Funding Open Access funding provided by The University of Osaka. This study was funded by JST (QiSS: JPMJOP1721) and AMED (22ck0106577h000, JP23ym0126091).

Data availability The datasets used and/or analyzed in the current study are not publicly available due to patient privacy concerns but are available from the corresponding author on reasonable request.

Declarations

Ethics approval The study was approved by the institutional review board of the University of Osaka Hospital (approval number: 19066), adhered to the Declaration of Helsinki.

Consent for publication Not applicable.

Consent to participate Written informed consent was obtained from all participants.

Conflict of interest FLG is an advisor at ABX, SOFIE Biosciences, Telix Pharma, Rhine pharma, and α-Fusion and has a patent application for PSMA-GCK01 and PSMA-1007. RAW has received speaker honoraria from and reports advisory board work for Novartis/AAA.

References

1. Foundation RP. Cancer Statistics in Japan. 2025. https://ganjoho.jp/public/qa_links/report/statistics/2025_jp.html
2. Chiu L, Lawhn-Heath C, Behr S, et al. Factors predicting metastatic disease in 68Ga-PSMA-11 PET positive osseous lesions in prostate cancer. J Nucl Med. 2020. https://doi.org/10.2967/jnumed.119.241174.
3. Toriihara A, Nobashi T, Baratto L, et al. Comparison of 3 interpretation criteria for 68Ga-PSMA11 PET based on inter- and intrareader agreement. J Nucl Med. 2020;61:533–9. https://doi.org/10.2967/jnumed.119.232504.
4. Giesel F, Hadaschik B, Cardinale J, et al. F-18 labelled PSMA-1007: Biodistribution, radiation dosimetry and histopathological validation of tumor lesions in prostate cancer patients. Eur J Nucl Med Mol Imaging. 2017;44:678–88. https://doi.org/10.1007/s00259-016-3573-4.
5. Malaspina S, Anttinen M, Taimen P, et al. Prospective comparison of 18F-PSMA-1007 PET/CT, whole-body MRI and CT in primary nodal staging of unfavourable intermediate- and high-risk prostate cancer. Eur J Nucl Med Mol Imaging. 2021;48:2951–9. https://doi.org/10.1007/s00259-021-05296-1.
6. Anttinen M, Ettala O, Malaspina S, et al. A prospective comparison of 18F-prostate-specific membrane antigen-1007 positron emission tomography computed tomography, whole-body 1.5 T magnetic resonance imaging with diffusion-weighted imaging, and single-photon emission computed tomography/computed tomography with traditional imaging in primary distant metastasis staging of prostate cancer (PROSTAGE). Eur Urol Oncol. 2021;4:635–44. https://doi.org/10.1016/j.euo.2020.06.012.
7. Lawal I, Ndlovu H, Kgatle M, et al. Prognostic value of PSMA PET/CT in prostate cancer. Semin Nucl Med. 2024;54:46–59. https://doi.org/10.1053/j.semnuclmed.2023.07.003.
8. Puik JR, Le C, Kazemier G, et al. Prostate-specific membrane antigen as target for vasculature-directed therapeutic strategies in solid tumors. Crit Rev Oncol Hematol. 2025;205:104556. https://doi.org/10.1016/j.critrevonc.2024.104556.
9. Werner R, Hartrampf P, Fendler W, et al. Prostate-specific Membrane Antigen Reporting and Data System Version 2.0. Eur Urol. 2023;84:491–502. https://doi.org/10.1016/j.eururo.2023.06.008.
10. Seifert R, Emmett L, Rowe S, et al. Second version of the prostate cancer molecular imaging standardized evaluation framework including response evaluation for clinical trials (PROMISE V2). Eur Urol. 2023;83:405–12. https://doi.org/10.1016/j.eururo.2023.02.002.
11. Ceci F, Oprea-Lager D, Emmett L, et al. E-PSMA: The EANM standardized reporting guidelines v1.0 for PSMA-PET. Eur J Nucl Med Mol Imaging. 2021;48:1626–38. https://doi.org/10.1007/s00259-021-05245-y.
12. Ma L, Hao Y, Zhai L, et al. Which PSMA PET/CT interpretation criteria most effectively diagnose prostate cancer? a retrospective cohort study. BMC Med Imaging. 2025;25. https://doi.org/10.1186/s12880-025-01557-9.
13. Jiao J, Kang F, Zhang J, et al. Establishment and prospective validation of an SUVmax cutoff value to discriminate clinically significant prostate cancer from benign prostate diseases in patients with suspected prostate cancer by 68Ga-PSMA PET/CT: a real-world study. Theranostics. 2021;11:8396–411. https://doi.org/10.7150/thno.58140.
14. Luo L, Zheng A, Chang R, et al. Evaluating the value of 18F-PSMA-1007 PET/CT in the detection and identification of prostate cancer using histopathology as the standard. Cancer Imaging. 2023. https://doi.org/10.1186/s40644-023-00627-x.
15. Masselli G, Sollaku S, De Angelis C, et al. 68Ga-PSMA PET/CT in recurrent prostate cancer after radical prostatectomy using PSMA-RADS Version 2.0. Diagnostics. 2024. https://doi.org/10.3390/diagnostics14121291.
16. Derwael C, Lavergne O, Lovinfosse P, et al. Interobserver agreement of [68Ga]Ga-PSMA-11 PET/CT images interpretation in men with newly diagnosed prostate cancer. EJNMMI Res. 2020;10. https://doi.org/10.1186/s13550-020-0596-4.
17. Herrmann K, Walz J, MacLennan S, et al. SPARC: The Standardised Prostate-specific Membrane Antigen Positron Emission Tomography/Computed Tomography Analysis and Reporting Consensus: A Delphi Analysis. Eur Urol. 2025. https://doi.org/10.1016/j.eururo.2025.08.005.
18. Watabe T, Uemura M, Soeda F, et al. High detection rate in [18F] PSMA-1007 PET: interim results focusing on biochemical recurrence in prostate cancer patients. Ann Nucl Med. 2021;35:523–8. https://doi.org/10.1007/s12149-021-01602-x.
19. Mainta IC, Neroladaki A, Wolf NB, et al. [(68)Ga]Ga-PSMA-11 PET and prostate cancer bone metastases: diagnostic performance of available standardized criteria. J Nucl Med. 2024;65:1376–82. https://doi.org/10.2967/jnumed.124.267899.
20. Yin Y, Werner R, Higuchi T, et al. Follow-up of lesions with equivocal radiotracer uptake on PSMA-targeted PET in patients with prostate cancer: predictive values of the PSMA-RADS-3A and PSMA-RADS-3B categories. J Nucl Med. 2019;60:511–6. https://doi.org/10.2967/jnumed.118.217653.
21. Letang A, Crombé A, Rousseau C, et al. Bone uptake in prostate cancer patients diagnostic performances of PSMA-RADS v1.0, clinical, biological, and 68Ga-PSMA-11 PET features to predict metastasis after biochemical recurrence. Clin Nucl Med. 2022;47:E529–39. https://doi.org/10.1097/RLU.0000000000004259.
22. Almalki Y, Basha M, Ali S, et al. Comparison of Prostate-specific Membrane Antigen Reporting and Data System Version 1.0 versus 2.0 for prostate cancer assessment. Radiol Imaging Cancer. 2025. https://doi.org/10.1148/rycan.240390.

23. Emmett L, Buteau J, Papa N, et al. The additive diagnostic value of prostate-specific membrane antigen positron emission tomography computed tomography to multiparametric magnetic resonance imaging triage in the diagnosis of prostate cancer (PRIMARY): a prospective multicentre study. Eur Urol. 2021;80:682–9. https://doi.org/10.1016/j.eururo.2021.08.002.
24. Emmett L, Papa N, Buteau J, et al. The PRIMARY Score: Using Intraprostatic (68)Ga-PSMA PET/CT Patterns to Optimize Prostate Cancer Diagnosis. J Nucl Med. 2022;63:1644–50. https://doi.org/10.2967/jnumed.121.263448.
25. Hofman M, Lawrentschuk N, Francis R, et al. Prostate-specific membrane antigen PET-CT in patients with high-risk prostate cancer before curative-intent surgery or radiotherapy (proPSMA): a prospective, randomised, multicentre study. LANCET. 2020;395:1208–16. https://doi.org/10.1016/S0140-6736(20)30314-7.
26. Giesel F, Knorr K, Spohn F, et al. Detection efficacy of 18F-PSMA-1007 PET/CT in 251 patients with biochemical recurrence of prostate cancer after radical prostatectomy. J NUCL MED. 2019;60:362–8. https://doi.org/10.2967/jnumed.118.212233.
27. Fendler WP, Weber M, Iravani A, et al. Prostate-Specific Membrane Antigen ligand positron emission tomography in men with nonmetastatic castration-resistant prostate cancer. CLIN CANCER RES. 2019;25:7448–54. https://doi.org/10.1158/1078-0432.CCR-19-1050.
28. Zhao G, Ji B. Head-to-head comparison of 68Ga-PSMA-11 PET/CT and 99mTc-MDP bone scintigraphy for the detection of bone metastases in patients with prostate cancer: a meta-analysis. AJR AM J ROENTGENOL. 2022;219:386–95. https://doi.org/10.2214/AJR.21.27323.
29. Yang B, Dong H, Zhang S, et al. PSMA PET vs. mpMRI for lymph node metastasis of prostate cancer: a systematic review and head-to-head comparative meta-analysis. ACAD RADIOL. 2025;32:2797–814. https://doi.org/10.1016/j.acra.2024.11.029.
30. Fendler W, Calais J, Eiber M, et al. Assessment of 68Ga-PSMA-11 PET accuracy in localizing recurrent prostate cancer: a prospective single-arm clinical trial. JAMA ONCOL. 2019;5:856–63. https://doi.org/10.1001/jamaoncol.2019.0096.
31. Perera M, Papa N, Roberts M, et al. Gallium-68 Prostate-specific Membrane Antigen positron emission tomography in advanced prostate cancer-updated diagnostic utility, sensitivity, specificity, and distribution of Prostate-specific Membrane Antigen-avid lesions: a systematic review and meta-analysis. EUR UROL. 2020;77:403–17. https://doi.org/10.1016/j.eururo.2019.01.049.
32. Burgard C, Hoffmann M, Frei M, et al. Detection efficacy of 68Ga-PSMA-11 PET/CT in biochemical recurrence of prostate cancer with very low PSA levels: a 7-year, two-center "Real-World" experience. Cancers. 2023. https://doi.org/10.3390/cancers15051376.
33. Grünig H, Maurer A, Thali Y, et al. Focal unspecific bone uptake on [18F]-PSMA-1007 PET: a multicenter retrospective evaluation of the distribution, frequency, and quantitative parameters of a potential pitfall in prostate cancer imaging. Eur J Nucl Med Mol Imaging. 2021;48:4483–94. https://doi.org/10.1007/s00259-021-05424-x.
34. Rizzo A, Morbelli S, Albano D, et al. The homunculus of unspecific bone uptakes associated with PSMA-targeted tracers: A systematic review-based definition. Eur J Nucl Med Mol Imaging. 2024;51:3753–64. https://doi.org/10.1007/s00259-024-06797-5.